Distributed Formation Control via Mixed Barycentric Coordinate and Distance-Based Approach

Kaveh Fathian, Dmitrii I. Rachinskii, Mark W. Spong, Tyler H. Summers, Nicholas R. Gans

***Abstract*— We present a distributed control strategy for a team of agents to autonomously achieve a desired planar formation. Our control strategy is based on combining the barycentric coordinate-based (BCB) and the distance-based (DB) approach. In the BCB approach, the almost global convergence of the agents to the desired formation shape is guaranteed, however, the formation scale cannot be controlled. In the DB method, the scale of the achieved formation is controlled, however, the convergence is local and in general stable undesired equilibria exist. By combining these methods via imposing a timescale separation between their respective dynamics, our proposed control strategy retains the advantages of each approach and avoids their shortcomings. We analyze the stability properties of the proposed control and prove that the desired formation is an almost globally stable equilibrium. We provide simulations to typify the theoretical results and compare our method with a leader-follower BCB (LF-BCB) approach that can be used to control the formation scale in the BCB strategy. In particular, we demonstrate that unlike the LF-BCB approach, our method is far more robust to measurement inaccuracies.**

***Index Terms*— Multi-agent systems, distributed formation control, agent-based systems.**

Supplementary Material

Video of paper summary and simulations is available at https://youtu.be/cYQ6ALUF83s. Simulations code can be download from https://goo.gl/QH5qhw.

I. Introduction

A formation of agents is a fundamental building block in applications such as the search and rescue missions [1], environmental mapping/monitoring [2], and cooperative object manipulation [3]. There exists a large body of work on formation control of autonomous agents [4]. While many methods rely on a centralized motion planning scheme or a global positioning/communication paradigm [5]–[8], fully distributed formation control strategies, such as the distance-based (DB) [9]–[11], bearing-based (BB) [12]–[15], and barycentric coordinate-based (BCB) [16]–[25] approach only require local relative measurements. Compared to the centralized methods, these distributed strategies have better scalability, naturally parallelized computation, and resiliency to global positioning signal jamming or loss.

In this work, we combine the BCB and the DB approach to derive a novel control strategy that has the advantages of both methods and avoids their shortcomings. A characteristic of the BCB approach is that the convergence of agents to the desired formation shape is guaranteed for almost all initial conditions. However, in the BCB (and the BB) approach, the scale of the formation cannot be controlled. In the existing DB approach, on the other hand, the scale of the formation is controllable, however, the convergence is not global and agents may attain an undesired shape. To control the scale of the formation in the BCB approach, the control can be modified to take a leader-follower (LF) form [16], in which by controlling the distance between a subset of agents (leaders) the scale of the remaining agents (followers) is controlled. However, as we will demonstrate by a simulation example, the LF-BCB approach can be very sensitive to inaccuracies and noise in the position measurements. Compared to the aforementioned methods, in our proposed approach the formation scale can be controlled, convergence is almost global, and the control is more robust to disturbances and inaccuracies in the measurements.

The main contribution of this work is the rigorous stability analysis of the proposed control, based on the mathematical machinery of slow-fast systems with timescale separation, which shows the almost global convergence of agents to the desired formation. The fast and slow dynamics in our proposed control correspond to the BCB and DB controls, respectively. To this day, no DB control strategy (for arbitrary numbers of agents and all feasible sensing graphs) with global or almost global convergence property is known in literature due to the existence of *undesired stable* equilibria discussed in [26]–[28]. Hence, this paper can be considered as the first result toward showing the existence of augmented DB controls with almost global convergence[1].

The paper is organized as follows. The notation and assumptions are introduced in Section II. In Section III, the BCB, DB, and LF-BCB control strategies are introduced and their properties are discussed. The proposed control strategy is presented in Sections IV, followed by the simulations in Section V. Additional remarks and future work are discussed in Section VI.

*This work was supported by the U.S. Air Force Research Laboratory grant FA8651-17-1-0001, the Army Research Office grant W911NF-17-1-0058, and the NSF grant DMS-1413223.

K. Fathian is with the Department of Aeronautics and Astronautics, Massachusetts Institute of Technology, Cambridge, MA, 02139 USA. E-mail: kavehf@mit.edu.

D. I. Rachinskii is with the Department of Mathematical Sciences, M. W. Spong is with the Department of Systems Engineering, T. H. Summers is with the Department of Mechanical Engineering, University of Texas at Dallas, Richardson, TX, 75080 USA. E-mail: {dmitry.rachinskiy, tyler.summers, mspong}@utdallas.edu.

N. R. Gans is with the UT Arlington Research Institute, University of Texas at Arlington, Arlington, TX, 76118 USA. E-mail: nick.gans@uta.edu.

[1]The global convergence in [29] is attained via inter-agent communication, which is not an assumption of this work or other DB literature.

II. Notation and Assumptions

We consider a team of $n \in \mathbb{N}$ agents with the inter-agent sensing topology described by an undirected graph $\mathcal{G} = (\mathcal{V}, \mathcal{E})$, where $\mathcal{V} = \mathbb{N}_n := \{1, 2, \ldots, n\}$ is the set of vertices, and $\mathcal{E} \subset \mathcal{V} \times \mathcal{V}$ is the set of edges. Each vertex of the graph represents an agent. An edge from vertex $i \in \mathcal{V}$ to $j \in \mathcal{V}$ indicates that agents i and j can measure the relative position of each other in their local coordinate frames. In such a case, agents i and j are called neighbors. The set of neighbors of agent i is denoted by $\mathcal{N}_i := \{j \in \mathcal{V} \,|\, (i,j) \in \mathcal{E}\}$.

Throughout this paper, we assume that the desired formation and the sensing topology are such that achieving the formation is physically feasible. In particular, we assume that the sensing topology is undirected and universally rigid. This assumption is both necessary and sufficient [17], [30] for guaranteeing the existence of control gains that lead to the desired formation.

III. Preliminaries

In this section, we review the BCB, DB, and LF-BCB formation control strategies for agents with the single-integrator dynamics. The motion of agents with single-integrator dynamics can be expressed as

$$\dot{q}_i = u_i, \tag{1}$$

where $q_i := [x_i, y_i]^\top \in \mathbb{R}^2$ represents the coordinates of agent $i \in \mathbb{N}_n$ in a global coordinate frame (unknown to the agent), and $u_i \in \mathbb{R}^2$ is the control law that is specified for agents by each strategy to achieve a desired formation. The control strategies discussed in this section are a cornerstone for our proposed control strategy that is discussed in the subsequent section.

A. The Barycentric Coordinate-Based Control Strategy

The BCB control strategy introduced by Lin et al. [16] is defined as

$$u_i := \sum_{j \in \mathcal{N}_i} A_{ij}\,(q_j - q_i), \tag{2}$$

where $q_j - q_i$ represent the relative position of agent j with respect to agent i, and $A_{ij} \in \mathbb{R}^{2\times 2}$ are constant control gain matrices that are designed and provided to agents before the mission and have the form

$$A_{ij} := \begin{bmatrix} a_{ij} & b_{ij} \\ -b_{ij} & a_{ij} \end{bmatrix}, \qquad a_{ij},\, b_{ij} \in \mathbb{R}. \tag{3}$$

Note that the diagonal elements of A_{ij} are identical, and off-diagonal elements only differ in sign. From the commutativity property of A_{ij} matrices (which holds due to their special structure) it follows that the closed-loop dynamics is invariant to expressing the coordinates in the global or local frames[2]. The geometric intuition behind the algebraic formulation of control strategy (2) is explained in the following example.

[2]Replacing global coordinates q_i^{global} with local coordinates $q_i^{\text{local}} = R\,q_i^{\text{global}} + T$ in (1) and (2) with R, T representing the relative rotation and translation between the local and global frames does not affect the dynamics since R, T are canceled.

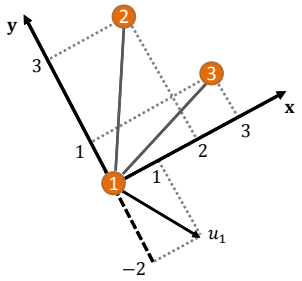

Fig. 1. Example of three agents with agents 2 and 3 neighbors of agent 1.

Example 1. Consider three agents in Fig. 1, and assume that agents 2 and 3 are neighbors of agent 1. That is, agent 1 can measure the position of agents 2 and 3 in its local coordinate frame. Denote by $q_2 = [2, 3]^\top$ and $q_3 = [3, 1]^\top$ the positions of the neighbors in agent 1's local coordinate frame, which itself is located at $q_1 = [0, 0]^\top$. Assume that control gain matrices

$$A_{12} = \begin{bmatrix} 2 & -1 \\ 1 & 2 \end{bmatrix}, \qquad A_{13} = \begin{bmatrix} -1 & 3 \\ -3 & -1 \end{bmatrix}, \tag{4}$$

are provided to agent 1 before the mission. From (2), the control vector for agent 1 in the current instance of time is computed as

$$u_1 = A_{12}\,(q_2 - q_1) + A_{13}\,(q_3 - q_1) = \begin{bmatrix} 1 \\ -2 \end{bmatrix}, \tag{5}$$

which is plotted in the figure. From the single-integrator dynamics (1) it follows that agent 1 moves along the vector u_1 with a speed equal to its magnitude. Matrices A_{12}, A_{13} can be interpreted as scaled rotation matrices that rotate and scale vectors that connect agent 1 to its neighbors. One can see that these actions are independent of the local coordinate frame's position and orientation in the global frame. Hence, q_2 and q_3 can be represented in either global or local coordinate frames.

By substituting (2) in (1), the closed-loop dynamics of the agents can be collectively expressed as

$$\dot{q} = A\,q, \tag{6}$$

where $q := [q_1^\top, q_2^\top, \ldots, q_n^\top]^\top \in \mathbb{R}^{2n}$ denote the aggregate position vector, and $A \in \mathbb{R}^{2n\times 2n}$ is the aggregate gain matrix given by

$$A = \begin{bmatrix} -\sum_{j\neq 1} A_{1j} & A_{12} & \cdots & A_{1n} \\ A_{21} & -\sum_{j\neq 2} A_{2j} & \cdots & A_{2n} \\ \vdots & & \ddots & \vdots \\ A_{n1} & A_{n2} & \cdots & -\sum_{j\neq n} A_{nj} \end{bmatrix}, \tag{7}$$

in which for $j \notin \mathcal{N}_i$ (i.e., when agents are not neighbors) the A_{ij} blocks are defined as zeros. Note that the 2×2 diagonal blocks of A are the negative sum of the rest of the blocks on the same row. Hence, A has a block Laplacian structure,

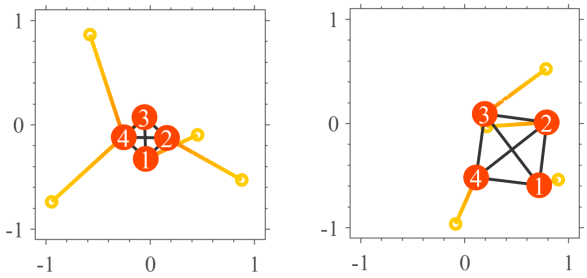

Fig. 2. Trajectories of 4 agents with a unit square desired formation under the BCB control. The desired formation shape is achieved, but the formation scale cannot be controlled.

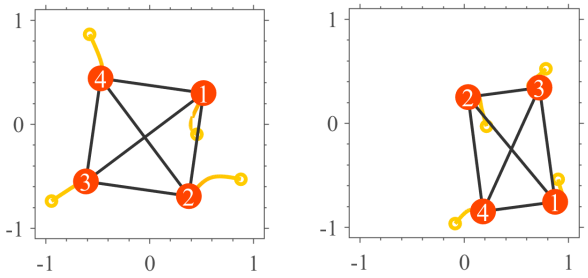

Fig. 3. Trajectories of 4 agents with a unit square desired formation under the DB control. (Left) Agents achieve the desired formation. (Right) Agents converge to an undesired stable equilibrium.

from which it follows that vectors

$$\begin{aligned} \mathbf{1} &:= [1,\, 0,\, 1,\, 0,\, \ldots,\, 1,\, 0]^\top \in \mathbb{R}^{2n} \\ \bar{\mathbf{1}} &:= [0,\, 1,\, 0,\, 1,\, \ldots,\, 0,\, 1]^\top \in \mathbb{R}^{2n} \end{aligned} \tag{8}$$

are in the kernel[3] of A.

Consider an embedding of the desired formation shape at an arbitrary location and orientation in the global coordinate frame. Let $q_i^* \in \mathbb{R}^2$ denote the coordinates of agent i at this embedding, and further denote by $\bar{q}_i^* \in \mathbb{R}^2$ coordinates rotated 90 degrees about the origin[4]. Let

$$\begin{aligned} q^* &:= [q_1^{*\top},\, q_2^{*\top},\, \ldots,\, q_n^{*\top}]^\top \in \mathbb{R}^{2n} \\ \bar{q}^* &:= [\bar{q}_1^{*\top},\, \bar{q}_2^{*\top},\, \ldots,\, \bar{q}_n^{*\top}]^\top \in \mathbb{R}^{2n} \end{aligned} \tag{9}$$

denote the aggregate coordinate vectors for all agents. The following theorem states the conditions that gain matrices must satisfy to ensure that the desired formation emerges from the interaction of all agents.

Theorem 1. *Consider agents with dynamics* (1) *and control* (2)*. Assume A_{ij} are such that in* (7)

(i) vectors $\mathbf{1}$, $\bar{\mathbf{1}}$, q^*, $\bar{q}^*$ form a basis for $\ker(A)$*,*

(ii) all nonzero eigenvalues of A have negative real parts,

then, agents almost globally converge to the desired formation shape (up to a rotation and a translation).

A formal proof for the case where A is symmetric is given in the Appendix. By noting that the closed-loop system (6) is a linear system, it is straightforward to see that under the conditions of Theorem 1 each trajectory converges to a point in $\ker(A)$, which consists of all rotations, translations, and scale factors of the desired formation coordinates. To give a geometric intuition, consider the unit square desired formation for 4 agents with a complete sensing graph. The trajectories of the agents under the BCB control (2) starting from two randomly generated initial conditions are shown in Fig. 2. As can be seen, the desired formation shape is achieved in both cases, however, the scale of the formation differs for each case.

Remark 1. *The null vectors $\mathbf{1}, \bar{\mathbf{1}}$ correspond to the case where all agents coincide. It can be shown that the set of initial conditions that converge to this coinciding equilibrium is measure zero. Hence, the convergence results in Theorem 1 is "almost" global. In practice, the trajectory of agents cannot remain on a measure zero set (due to noise, disturbances, etc.), and such cases are not of practical concern.*

Remark 2. *For the existence of A_{ij} that satisfy the conditions of Theorem 1, it is both necessary and sufficient that the sensing graph among agents is 2-rooted. In addition, for matrix A in* (7) *to be symmetric the sensing graph must be undirected and universally rigid. These conditions have been derived in [18, Thm. 3.2], and we assume they hold throughout this paper*[5].

We emphasize that the strength of the BCB approach is the almost *global* convergence of the agent to the desired formation shape, while the downside is that the formation scale cannot be controlled and depends on the initial positions of the agents. Lastly, gain matrices for which A is symmetric and conditions of Theorem 1 are satisfied can be computed by solving a semidefinite program (SDP) that is presented in our previous work [31], [32].

B. The Distance-Based Control Strategy

An alternative approach to achieve the desired formation is the DB strategy defined by

$$u_i := \sum_{j \in \mathcal{N}_i} (d_{ij} - d_{ij}^*)\,(q_j - q_i), \tag{10}$$

where $d_{ij} := \|q_j - q_i\|$ denotes the distance between agents i and j, and $d_{ij}^* \in \mathbb{R}$ denotes its corresponding value in the desired formation. Intuitively, the role of each $(d_{ij} - d_{ij}^*)\,(q_j - q_i)$ term in (10) is to pull agent i toward its neighbor j when the distance d_{ij} between them is larger than the desired distance d_{ij}^*, and vice versa.

Proposition 1. *Consider agents with dynamics* (1) *and control* (10)*. If the desired formation is infinitesimally rigid [33], then the desired formation is a locally stable equilibrium (up to a rotation and a translation).*

The proof of Proposition 1 is given in [10, Thm. 13]. Note that unlike the BCB approach, in the DB control strategy convergence to the desired formation is only guaranteed *locally* since in general undesired *stable* equilibria are present

[3]The kernel or null space of a matrix $A \in \mathbb{R}^{n\times n}$ is defined as $\ker(A) := \{v \in \mathbb{R}^n \mid A\,v = 0\}$.

[4]That is, if $q_i^* = [x_i,\, y_i]^\top$, then $\bar{q}_i^* := [-y_i,\, x_i]^\top$.

[5]These results are for general formation shapes. For some special shapes, the gains may exist even if the rigidity conditions are not satisfied.

[26]–[28]. As an example, consider the unit square desired formation for 4 agents with a complete sensing graph. The trajectories of agents under the DB control (10) are shown in Fig. 3, where the initial positions of the agents are chosen the same as in Fig. 2. As can be seen, the desired formation is achieved only in the left figure, and the agents converge to an undesired equilibrium from their initial positions in the right figure.

C. The Leader-Follower BCB Formulation

The LF-BCB formulation has been proposed in [16] to fix the formation scale in the BCB approach. The main idea consists of fixing the distance between two leader agents and hence forcing the remaining agents (followers) to converge to the formation with the desired scale. Let us assume, without loss of generality, that agents 1 and 2 are the leaders. The corresponding LF-BCB control is given by

$$\begin{aligned} u_1 &:= (d_{12} - d_{12}^*)(q_1 - q_2), \\ u_2 &:= (d_{12} - d_{12}^*)(q_2 - q_1), \\ u_i &:= \sum_{j \in \mathcal{N}_i} A_{ij}\,(q_j - q_i), \qquad i \geq 3. \end{aligned} \tag{11}$$

Similar to the DB strategy, the role of u_1 (or u_2) is to bring the distance d_{12} between the leaders to its desired value d_{12}^*. The control for the remaining follower agents u_i, $i \geq 3$ is the same as the BCB strategy (2).

Substituting (11) in (1) gives the aggregate closed-loop dynamics

$$\dot{q} = A\,q + \begin{bmatrix} g(q_1, q_2) \\ 0 \end{bmatrix}, \tag{12}$$

where $g : \mathbb{R}^2 \times \mathbb{R}^2 \to \mathbb{R}^4$ maps the coordinates of the leaders to control vectors u_1, u_2 according to (11), and the first 4 rows of A associated to the leader agents are zeros. Note that in (12), matrix A is *not* symmetric (in contrast to our proposed approach).

Proposition 2. *Consider agents with dynamics* (1) *and control* (11). *If A in* (12) *satisfies the conditions of Theorem 1, then, agents almost globally converge to the desired formation (up to a rotation and a translation).*

Proof of Proposition 2 is given in [16, Thm. 4.4] and hence is omitted here. As we will illustrate by an example in Section V, additive disturbances in the leader positions, which model measurement inaccuracies that exist in practice, can propagate and get amplified by the follower agents, hence, severely affecting the formation. Therefore, ideally, all agents should participate in controlling the distance to their neighbors and the LF-BCB approach should be avoided.

IV. The Proposed Control Strategy

We now present the main results of this paper. To achieve the desired formation shape with the desired scale, we combine the BCB (2) and the DB (10) control strategies according to

$$u_i = \sum_{j \in \mathcal{N}_i} A_{ij}\,(q_j - q_i) + \epsilon f(d_{ij} - d_{ij}^*)\,(q_j - q_i), \tag{13}$$

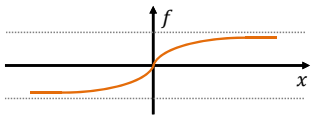

Fig. 4. Graph of function $f(x)$.

where $\epsilon > 0$ is a real scalar, and the bounded smooth map $f : \mathbb{R} \to \mathbb{R}$ is chosen such that $x\,f(x) > 0$ for $x \neq 0$, $f(0) = 0$, and $f'(0) > 0$, as illustrated in Fig. 4. Possible choices for f are $f : x \mapsto \arctan(x)$ or $f : x \mapsto \tanh(x)$. The role of f in (13) is to bound the magnitude of the DB control strategy.

The intuition behind the control strategy (13) is as follows. By choosing ϵ small, the BCB control drives the agents to the desired formation shape (fast dynamics). Once the agents are in a small neighborhood of the desired shape, the DB control contracts/expands the formation to achieve the desired scale (slow dynamics).

Theorem 2. *Consider agents with dynamics* (1) *and control* (13). *Assume A_{ij} matrices are such A in* (7) *is symmetric and satisfies the conditions of Theorem 1. Then, there exists $\epsilon^* > 0$ such that for all $0 < \epsilon < \epsilon^*$ the desired formation is an almost globally exponentially stable equilibrium.*

Proof of Theorem 2 is presented in the Appendix. The term "equilibrium" should be understood as the *set of equilibria*, which consists of all rotations and translations of the desired formation. Furthermore, the almost global exponential stability implies that almost every trajectory coverages to a point in this set with a rate that depends on the initial condition. As a combination of the BCB and DB control approach, the control strategy (13) has the advantages of both methods. Namely, convergence to the desired formation is almost global and the achieved formation has the desired scale.

Remark 3. *Theorem 2 ensures the existence of an ϵ, however, the value of ϵ^* is not specified. From the proof of Theorem 2, one can see that ϵ must be chosen small enough such that matrix G in* (29) *is negative definite. By considering the worst case scenario and using the Gershgorin circle theorem [34, Thm. 6.1.1], an upper bound for the largest eigenvalue of F in* (21) *can be derived as $\mu_{max} := 2\,(n-1)\,f_{\max}$, where n is the number of agents and $f_{\max} > 0$ is an upper bound for $|f(\cdot)|$ in* (13). *If $\lambda_{\max} < 0$ denote the largest (nonzero) eigenvalue of A, then by choosing*

$$\epsilon < |\lambda_{\max}/\mu_{\max}| \tag{14}$$

the negative definiteness of G is guaranteed from the Weyl Theorem [34, Thm. 4.3.1].

Lastly, it can be shown that under (13) the closed-loop dynamics is globally *stable* (i.e., trajectories are bounded) for all values of ϵ and the only consequence of choosing a large ϵ that does not satisfy (14) is the possibility of convergence to an undesired equilibrium associated with the DB approach.

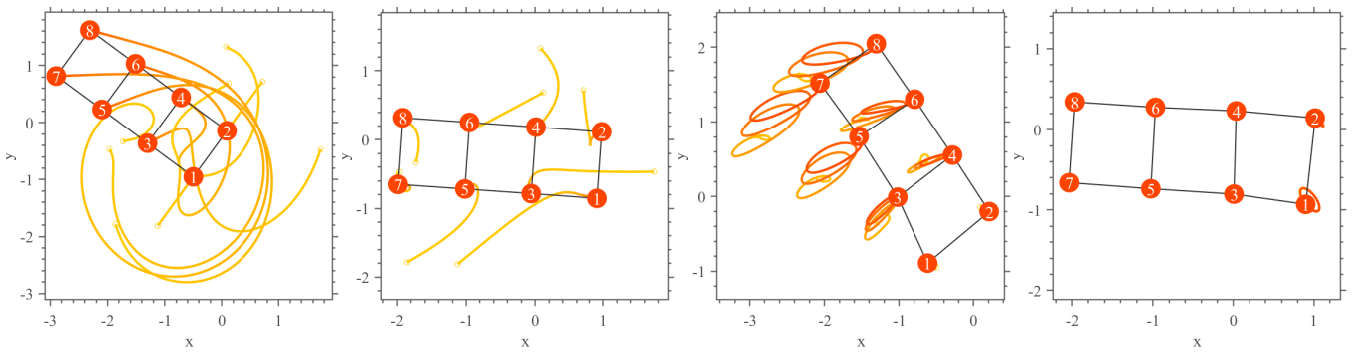

(a) (b) (c) (d)

Fig. 5. Trajectories of 8 agents with a rectangular desired formation. (a) Trajectories under the LF-BCB control (11). (b) Trajectories under the proposed control (13). (c) Effect of additive disturbances to the positions of agents 1 and 2 on the formation shape under the LF-BCB control. (d) Effect of additive disturbances under the proposed control.

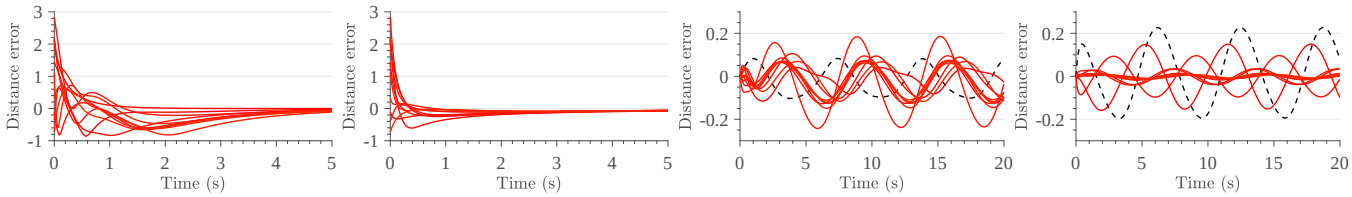

(a) (b) (c) (d)

Fig. 6. Distance errors $d_{ij} - d^*_{ij}$ plotted versus time for all agents and their neighbors. (a) Errors corresponding to the LF-BCB control. (b) Errors corresponding to the proposed control. (c) Effect of additive disturbances to the positions of agents 1 and 2 on the inter-agent distance errors under the LF-BCB control. The distance error between agents 1 and 2 is shown via the dashed line. (d) Effect of additive disturbances under the proposed control.

V. Simulations

We present two simulations to validate the proposed approach and compare the sensitivity of the discussed methods to disturbances. Links to the Matlab simulation code and videos are provided in the Supplementary Material section.

The desired formation considered in the simulations is a rectangular formation with 8 agents (see Fig. 5(b)), where the desired distance among all neighboring agents is defined as 1 unit of measurements. The gain matrices that satisfy the conditions of Theorem 1 for the corresponding desired formation are computed using the SDP approach presented in our previous work [31], [32]. The algorithm discussed in [16] is used to compute the gain matrices that satisfy the conditions of Proposition 2 for the LF-BCB approach. To have a fair comparison, the aggregate gain matrices computed from both approaches are designed to have the same eigenvalues. In particular, the eigenvalues of matrix A for both methods are $\{-0.72, -2.68, -5.36, -5.36, -8.04, -10\}$, each with multiplicity two[6]. The value of ϵ in the proposed control strategy (13) is set to 0.5.

Figs. 5(a) and (b) show the trajectories of agents starting from the same randomly chosen initial positions under the LF-BCB control strategy (11) and the proposed strategy (13), respectively. The corresponding distance errors defined as $d_{ij} - d^*_{ij}$ between agents and their neighbors are plotted versus time in Figs. 6(a), (b). As can be seen from the figures, the agents achieve the desired formation with the desired scale under both control strategies. However, the traversed trajectories are much shorter under our proposed control strategy[7].

To test the sensitivity of control strategies to noise and measurement inaccuracies that often exist in a practical implementation, periodic disturbances of $0.2\,[\sin(t),\ \cos(t)]^\top$ and $0.1\,[\cos(t),\ \sin(t)]^\top$ are added to the position vectors q_1 and q_2, respectively. The effect of these additive disturbances on the formation shape are shown in Figs. 5(c), (d) for the LF-BCB and the proposed control strategy, respectively. The corresponding inter-agent distance errors are plotted in Figs. 6(c), (d). As can be seen from the figures, in the LF-BCB control approach the additive disturbance is amplified by the follower agents. In particular, the further a follower agent is from the leaders, the more severe is the effect of the disturbance on the agent's trajectory. Under the proposed control, on the other hand, the disturbance is attenuated and agents that are further from the disturbed agents are less affected.

VI. Concluding Remarks and Future Work

By combining the BCB and DB control strategies using the slow-fast dynamics, we presented a novel distributed formation control that has the advantages of both methods and avoids their shortcomings. In particular, similar to the BCB and unlike the DB approach, the agents almost globally

[6]All numbers are rounded up to two decimal digits.

[7]We point out that simulation with $\epsilon < 0.5$ did not lead to a noticeably different trajectory. Although the convergence to the desired scale was slower, the length of the traversed trajectories remained roughly the same.

coverage to the desired formation. On the other hand, similar to the DB and unlike the BCB approach, the formation scale can be controlled. Moreover, under the proposed strategy the formation is far more robust to disturbances that affect the LF-BCB approach.

As discussed in our previous work [23], [31], [32], the BCB control with gains designed from the SDP method enjoys several robustness properties. Specifically, any positive scaling or rotation (up to $\pm 90^\circ$) of the control vector, saturation of the control magnitude, and switching among the feasible sensing topologies do not affect the convergence of the agents to the desired formation. Furthermore, a fully distributed collision avoidance algorithm emerges naturally from these robustness properties. Since the fast dynamics associated with the control proposed in this work is based on the BCB approach, one can expect the same properties to follow. Detailed analysis of these properties will be a topic of future work. We further point out that although the focus of this paper was on agents with the single-integrator dynamics, one can leverage [31], [32] to extend the results to higher-order dynamics.

The results of this work were established for planar formations and undirected sensing graphs. Additional future work includes extending the results to 3D formations and directed graphs. The observation that disturbances and measurement inaccuracies in leader positions can strongly affect the shape of the formation in the LF-BCB approach was demonstrated using a simulation example. Quantifying the effect of disturbances in the LF-BCB approach analytically is another topic of research.

APPENDIX

We first prove Theorem 1 for *symmetric* A since a similar procedure is used subsequently to prove Theorem 2.

***Proof** (Theorem 1).* Let $N := [q^*,\, \bar{q}^*,\, \mathbf{1},\, \bar{\mathbf{1}}] \in \mathbb{R}^{2n\times 4}$ denote the bases for $\ker(A)$. Further, let $U\,S\,V^\top = N$ be the (full) singular value decomposition (SVD) of N, where

$$U = [\bar{Q},\ Q] \ \in \mathbb{R}^{2n\times 2n}, \tag{15}$$

with columns of $\bar{Q} \in \mathbb{R}^{2n\times 4}$ denoting orthonormal vectors that span $\ker(A)$, and columns of $Q \in \mathbb{R}^{2n\times(2n-4)}$ denoting orthonormal vectors that are the orthogonal complement of $\bar{Q}$. Consider the change of coordinates defined by $p := U^\top q$, in which the closed-loop dynamics $\dot{q} = A\,q$ is

$$\begin{aligned}\dot{p} &= U^\top A\,U\,p \\ &= \begin{bmatrix}\bar{Q}^\top \\ Q^\top\end{bmatrix} A\ \begin{bmatrix}\bar{Q} & Q\end{bmatrix} p = \begin{bmatrix}\bar{Q}^\top A\,\bar{Q} & \bar{Q}^\top A\,Q \\ Q^\top A\,\bar{Q} & Q^\top A\,Q\end{bmatrix} p. \end{aligned} \tag{16}$$

Let $p := [p_1^\top,\ p_2^\top]^\top$, where $p_1 \in \mathbb{R}^4$ represents the first 4 elements of p, and $p_2 \in \mathbb{R}^{2n-4}$ is the vector of remaining elements. Since $\bar{Q}$ is a basis for $\ker(A)$ and A is symmetric, we have $\bar{Q}^\top A = A\bar{Q} = 0$, and from (16)

$$\begin{bmatrix}\dot{p}_1 \\ \dot{p}_2\end{bmatrix} = \begin{bmatrix}0 & 0 \\ 0 & Q^\top A\,Q\end{bmatrix} \begin{bmatrix}p_1 \\ p_2\end{bmatrix}. \tag{17}$$

The eigenvalues of $Q^\top A\,Q \ \in \mathbb{R}^{(2n-4)\times(2n-4)}$ are the same as the eigenvalues of A that are not associated to the kernel vectors. From condition (ii) in the theorem, these eigenvalues have negative real parts, and therefore $p_2 \to 0$ as $t \to \infty$, while p_1 remains constant. Hence,

$$\lim_{t\to\infty} q = \lim_{t\to\infty} U\,p = \begin{bmatrix}\bar{Q} & Q\end{bmatrix} \begin{bmatrix}p_1 \\ 0\end{bmatrix} = \bar{Q}\,p_1, \tag{18}$$

which shows each trajectory converge to a point in $\ker(A)$. □

The following Lemma is used in the proof of Theorem 2.

Lemma 1. *[35, Thm. 11.4] Consider the singularly perturbed system*

$$\begin{aligned}\dot{x} &= f(t,\, x,\, z,\, \epsilon), \\ \epsilon\,\dot{z} &= g(t,\, x,\, z,\, \epsilon),\end{aligned} \tag{19}$$

where $x \in B_r \subset \mathbb{R}^n$, with B_r representing the ball of radius r about the origin, and $z \in \mathbb{R}^m$. Assume that for all $(t,\, x,\, \epsilon) \in [0,\, \infty) \times B_r \times [0,\, \epsilon_0]$ it holds that

- *(i) $f(t,\, 0,\, 0,\, \epsilon) = 0$ and $g(t,\, 0,\, 0,\, \epsilon) = 0$.*
- *(ii) The equation $g(t,\, x,\, z,\, 0) = 0$ has an isolated root $z = h(t, x)$ such that $h(t, 0) = 0$.*
- *(iii) The functions $f,\, g,\, h$, and their partial derivatives up to the second order are bounded for $z - h(t, x) \in B_\rho \subset \mathbb{R}^m$.*
- *(iv) The origin of the reduced system $\dot{x} = f(t,\, x,\, h(t, x),\, 0)$ is exponentially stable.*
- *(v) The origin of the boundary-layer system $\frac{dy}{d\tau} = g(t,\, x,\, y + h(t, x),\, 0)$, where $\tau = \epsilon\,t$, is exponentially stable, uniformly in $(t,\, x)$.*

Then, there exists $\epsilon^* > 0$ such that for all $\epsilon < \epsilon^*$, then origin of (19) *is exponentially stable.*

Remark 4. *In Lemma 1, if $B_r = \mathbb{R}^n$, $B_\rho = \mathbb{R}^m$, and the reduced and the boundary-later systems are globally stable, from the proof presented in [35, Thm. 11.4] one can conclude that the stability results hold globally, i.e., all trajectories converge to the origin. This observation is used in the following analysis.*

Based on the procedure discussed in the proof of Theorem 1, we now present the proof of Theorem 2.

***Proof** (Theorem 2).* The closed-loop dynamics of single-integrator agents under control law (13) is given by

$$\dot{q} = A\,q + \epsilon\,F(q)\,q \tag{20}$$

where $F(q) : \mathbb{R}^{2n} \to \mathbb{R}^{2n\times 2n}$ is defined as

$$F(q) = \begin{bmatrix} -\sum_{j\neq 1} F_{1j} & F_{12} & \cdots & F_{1n} \\ F_{21} & -\sum_{j\neq 2} F_{2j} & \cdots & F_{2n} \\ \vdots & & \ddots & \vdots \\ F_{n1} & F_{n2} & \cdots & -\sum_{j\neq n} F_{nj} \end{bmatrix}, \tag{21}$$

with 2×2 off-diagonal block elements

$$F_{ij} := \begin{cases} f(d_{ij} - d_{ij}^*)\,I & \text{if } j \in \mathcal{N}_i \\ 0 & \text{otherwise} \end{cases} \tag{22}$$

where $I \in \mathbb{R}^{2\times 2}$ is the identity matrix.

Consider the change of coordinates $p := U^\top q$ defined in the proof of Theorem 1, where $U = [\bar{Q},\ Q]$ with columns of $\bar{Q} \in \mathbb{R}^{2n\times 4}$ denoting orthonormal vectors that span $\ker(A)$. In particular, $\bar{Q}$ can be chosen as $\bar{Q} = [\bar{Q}_1,\ \bar{Q}_2]$ with[8]

$$\bar{Q}_1 := \begin{bmatrix} \frac{q^*}{\|q^*\|}, & \frac{\bar{q}^*}{\|\bar{q}^*\|} \end{bmatrix} \in \mathbb{R}^{2n\times 2},\ \bar{Q}_2 := \begin{bmatrix} v_1, & v_2 \end{bmatrix} \in \mathbb{R}^{2n\times 2}, \tag{23}$$

where $v_1,\ v_2 \in \mathbb{R}^{2n}$ are orthonormal vectors that span $\mathbf{1},\ \bar{\mathbf{1}}$ and are orthogonal to $\bar{Q}_1$. In the new coordinates, the closed-loop dynamics (20) is given by

$$\begin{bmatrix} \dot{p}_1 \\ \dot{p}_2 \end{bmatrix} = \begin{bmatrix} 0 & 0 \\ 0 & Q^\top A\, Q \end{bmatrix} \begin{bmatrix} p_1 \\ p_2 \end{bmatrix} + \epsilon \begin{bmatrix} \bar{Q}^\top F\, \bar{Q} & \bar{Q}^\top F\, Q \\ Q^\top F\, \bar{Q} & Q^\top F\, Q \end{bmatrix} \begin{bmatrix} p_1 \\ p_2 \end{bmatrix}, \tag{24}$$

where $F(q)$ is denoted by F for brevity. Due to the block Laplacian structure of F, which implies $F\,\mathbf{1} = F\,\bar{\mathbf{1}} = 0$, by using the bases vectors defined in (23) it follows that

$$\bar{Q}^\top F\, \bar{Q} = \begin{bmatrix} \lambda I & 0 \\ 0 & 0 \end{bmatrix} \in \mathbb{R}^{4\times 4}, \quad \bar{Q}^\top F\, Q = \begin{bmatrix} H^\top \\ 0 \end{bmatrix} \in \mathbb{R}^{4\times 2n}, \tag{25}$$

where $I \in \mathbb{R}^{2\times 2}$ is the identity matrix, and $\lambda(p) : \mathbb{R}^{2n} \to \mathbb{R}$, $H(p) : \mathbb{R}^{2n} \to \mathbb{R}^{2n\times 2}$ are defined as

$$\lambda := \frac{1}{\|q^*\|^2}\, q^{*\top} F\, q^* = \frac{1}{\|\bar{q}^*\|^2}\, \bar{q}^{*\top} F\, \bar{q}^*, \tag{26}$$

$$H := Q^\top F\, \bar{Q}_1, \tag{27}$$

where for brevity we omitted the dependency of λ and H on p. Let us denote the components of $p_1 \in \mathbb{R}^4$ by $p_1 = [p_{11}^\top,\ p_{12}^\top]^\top$, $p_{11},\ p_{12} \in \mathbb{R}^2$, where p_{11} is the component of state along the desired shape, and p_{12} is the translational component. From substituting (25) in (24) we get

$$\begin{aligned} \begin{bmatrix} \dot{p}_{11} \\ \dot{p}_{12} \end{bmatrix} &= \epsilon \begin{bmatrix} \lambda & 0 \\ 0 & 0 \end{bmatrix} \begin{bmatrix} p_{11} \\ p_{12} \end{bmatrix} + \epsilon \begin{bmatrix} H^\top \\ 0 \end{bmatrix} p_2 \\ \dot{p}_2 &= \epsilon \begin{bmatrix} H & 0 \end{bmatrix} \begin{bmatrix} p_{11} \\ p_{12} \end{bmatrix} + G\, p_2 \end{aligned} \tag{28}$$

where G is defined as

$$G := Q^\top A\, Q + \epsilon\, Q^\top F\, Q \in \mathbb{R}^{(2n-4)\times(2n-4)}. \tag{29}$$

Since $Q^\top A\, Q$ is negative definite by assumption, for ϵ small enough from the boundedness of $\|F\|$ (which holds due to the boundedness of its elements) G remains negative definite [34, Thm. 6.3.2]. Furthermore, from (28) we have $\dot{p}_{12} = 0$, which shows that p_{12} remains constant. Hence, by disregarding p_{12} in (28) the remaining dynamics can be written as

$$\begin{aligned} \dot{p}_{11} &= \epsilon\, \lambda\, p_{11} + \epsilon H^\top p_2, \\ \dot{p}_2 &= \epsilon\, H\, p_{11} + G\, p_2. \end{aligned} \tag{30}$$

By representing (30) in the new time scale $\tau = \epsilon\, t$, which implies $\frac{d}{dt} = \epsilon\, \frac{d}{d\tau}$, we get

$$\begin{aligned} \epsilon\, \frac{d\, p_{11}}{d\tau} &= \epsilon\, \lambda\, p_{11} + \epsilon\, H^\top p_2, \\ \epsilon\, \frac{d\, p_2}{d\tau} &= \epsilon\, H\, p_{11} + G\, p_2. \end{aligned} \tag{31}$$

[8]Recall from Theorem 1 (i) that $\|q^*\|, \|\bar{q}^*\| \neq 0$.

Canceling ϵ from both sides of the first equation yields

$$\begin{aligned} \dot{p}_{11} &= \lambda\, p_{11} + H^\top p_2, \\ \epsilon\, \dot{p}_2 &= \epsilon\, H\, p_{11} + G\, p_2, \end{aligned} \tag{32}$$

where for brevity $\dot{p}_{11},\ \dot{p}_2$ denote the time derivatives in the new time τ.

System (32) is in the singularly perturbed format of (19) in Lemma 1. Before applying the Lemma, we make the following remarks: 1) Our analysis is based on the desired formation equilibrium instead of the origin used in the Lemma[9]. Furthermore, this equilibrium represents all rotations of the desired formation on the plane. 2) The origin $q = 0$ (i.e., coinciding agents) is an equilibrium of (20). By linearizing (20) about this equilibrium, it can be shown that the corresponding Jacobian matrix, and hence the equilibrium, is unstable. It is straightforward to formulate a modification of Lemma 1 and Remark 4 to include the above remarks. Having this point in mind, we apply Lemma 1 directly on the system (32).

At the desired formation $q = q^*$, from $p = U^\top q$ we have $p_{11} = p_{11}^* := \bar{Q}_1^\top q^*$ and $p_2 = Q^\top q^* = 0$. Also, from (22) it follows that at the desired formation $F = 0$. Taking these into account, we proceed by showing that (32) satisfies the conditions of Lemma 1:

(i) Since at the desired formation $F = 0$, from (26) and (27) λ and H are zero. Thus, $p_{11} = p_{11}^*,\ p_2 = 0$ is an equilibrium of (32).

(ii) Setting $\epsilon = 0$ in (32) yields the quasi steady state equation $G\, p_2 = 0$. Since G is negative definite by assumption, $p_2 = 0$ is the unique isolated root of the quasi steady state equation.

(iii) By direct calculation, it is straightforward to show that the right hand sides of (32) have bounded second order derivatives for all $p_{11} \in \mathbb{R}^2,\ p_2 \in \mathbb{R}^{2n-4}$.

(iv) By substituting $p_2 = 0$ in (32) the reduced order dynamics is derived as

$$\dot{p}_{11} = \lambda\, p_{11}. \tag{33}$$

Note that $p_2 = 0$ implies that the agents are the desired formation shape, i.e., $p_{11} = c\, p_{11}^*$, where $c \geq 0$ is the scale of the formation. Since

$$\begin{cases} d_{ij} - d_{ij}^* < 0 & \text{if } c < 1 \\ d_{ij} - d_{ij}^* = 0 & \text{if } c = 1 \\ d_{ij} - d_{ij}^* > 0 & \text{if } c > 1 \end{cases} \tag{34}$$

from the definitions of F and λ in (21) and (26), and since $c = \|p_{11}\|/\|p_{11}^*\|$, it follows that

$$\begin{cases} \lambda > 0 & \text{if } \|p_{11}\| < \|p_{11}^*\| \\ \lambda = 0 & \text{if } \|p_{11}\| = \|p_{11}^*\| \\ \lambda < 0 & \text{if } \|p_{11}\| > \|p_{11}^*\| \end{cases} \tag{35}$$

as illustrated in Fig. 7. Equation (35) implies that the desired formation $p_{11} = p_{11}^*$ (corresponding to $c = 1$)

[9]This does not change the analysis since one can use the transformation $\tilde{q} := q - q^*$ to shift the equilibrium to the origin.

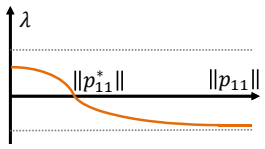

Fig. 7. Value of λ versus the formation scale $\|p_{11}\|$.

is an asymptotically stable equilibrium for (33) [35, see Example 4.2]. By direct computation, one can further show that the slope of λ at $c = 1$ is a strictly negative number, i.e., $\frac{d\lambda}{dc} = k\, f'(0) < 0$, where $k < 0$ is a constant scalar that depends on the desired formation coordinates q^*. Hence, the equilibrium $p_{11} = p_{11}^*$ is almost[10] globally exponentially stable [35, Thm. 4.13].

(v) Substituting $\epsilon = 0$ in (32) gives the boundary-layer system $\dot{p}_2 = G\, p_2$. From negative definiteness of G it follows that the origin is a globally exponentially stable equilibrium of the boundary-layer system.

Consequently, from Lemma 1 it follows that for ϵ small enough the desired formation is an exponentially stable equilibrium of system (20). From Remark 4, and due to the existence of an undesired but *unstable* equilibrium at the origin, the (nonuniform) exponential stability holds almost globally. □

REFERENCES

[1] T. Gunn and J. Anderson, "Dynamic heterogeneous team formation for robotic urban search and rescue," *Journal of Computer and System Sciences*, vol. 81, no. 3, pp. 553–567, 2015.

[2] H. Carrillo, P. Dames, V. Kumar, and J. A. Castellanos, "Autonomous robotic exploration using occupancy grid maps and graph slam based on shannon and rényi entropy," in *International Conference on Robotics and Automation*. IEEE, 2015, pp. 487–494.

[3] G. Habibi, Z. Kingston, W. Xie, M. Jellins, and J. McLurkin, "Distributed centroid estimation and motion controllers for collective transport by multi-robot systems," in *IEEE International Conference on Robotics and Automation*, 2015, pp. 1282–1288.

[4] K.-K. Oh, M.-C. Park, and H.-S. Ahn, "A survey of multi-agent formation control," *Automatica*, vol. 53, pp. 424–440, 2015.

[5] N. Michael, M. M. Zavlanos, V. Kumar, and G. J. Pappas, "Distributed multi-robot task assignment and formation control," in *IEEE International Conference on Robotics and Automation*, 2008, pp. 128–133.

[6] M. Aranda, G. López-Nicolás, C. Sagüés, and M. M. Zavlanos, "Coordinate-free formation stabilization based on relative position measurements," *Automatica*, vol. 57, pp. 11–20, 2015.

[7] N.-s. P. Hyun, P. A. Vela, and E. I. Verriest, "Collision free and permutation invariant formation control using the root locus principle," in *American Control Conference*, 2016, pp. 2572–2577.

[8] T. Motoyama and K. Cai, "Top-down synthesis of multi-agent formation control: An eigenstructure assignment based approach," in *American Control Conference*. IEEE, 2017, pp. 259–264.

[9] R. Olfati-Saber and R. M. Murray, "Distributed cooperative control of multiple vehicle formations using structural potential functions," in *IFAC World Congress*, 2002, pp. 346–352.

[10] L. Krick, M. E. Broucke, and B. A. Francis, "Stabilisation of infinitesimally rigid formations of multi-robot networks," *International Journal of Control*, vol. 82, no. 3, pp. 423–439, 2009.

[11] Y.-P. Tian and Q. Wang, "Global stabilization of rigid formations in the plane," *Automatica*, vol. 49, no. 5, pp. 1436–1441, 2013.

[12] M. Basiri, A. N. Bishop, and P. Jensfelt, "Distributed control of triangular formations with angle-only constraints," *Systems & Control Letters*, vol. 59, no. 2, pp. 147–154, 2010.

[13] M. Deghat and A. N. Bishop, "Distributed shape control and collision avoidance for multi-agent systems with bearing-only constraints," in *European Control Conference*. IEEE, 2015, pp. 2342–2347.

[14] S. Zhao and D. Zelazo, "Bearing rigidity and almost global bearing-only formation stabilization," *IEEE Transactions on Automatic Control*, vol. PP, no. 99, pp. 1–1, 2015.

[15] M. H. Trinh, S. Zhao, Z. Sun, D. Zelazo, B. D. Anderson, and H.-S. Ahn, "Bearing-based formation control of a group of agents with leader-first follower structure," *IEEE Transactions on Automatic Control*, 2018.

[16] Z. Lin, L. Wang, Z. Han, and M. Fu, "Distributed formation control of multi-agent systems using complex laplacian," *IEEE Transactions on Automatic Control*, vol. 59, no. 7, pp. 1765–1777, July 2014.

[17] Z. Lin, L. Wang, Z. Han, and v. Minyue Fu, "A graph laplacian approach to coordinate-free formation stabilization for directed networks," *IEEE Transactions on Automatic Control*, vol. 61, no. 5, pp. 1269–1280, May 2016.

[18] Z. Lin, L. Wang, Z. Chen, M. Fu, and Z. Han, "Necessary and sufficient graphical conditions for affine formation control," *IEEE Transactions on Automatic Control*, vol. 61, no. 10, pp. 2877–2891, 2016.

[19] A. N. Bishop, T. H. Summers, and B. D. Anderson, "Stabilization of stiff formations with a mix of direction and distance constraints," in *IEEE International Conference on Control Applications*, 2013, pp. 1194–1199.

[20] A. N. Bishop, M. Deghat, B. Anderson, and Y. Hong, "Distributed formation control with relaxed motion requirements," *International Journal of Robust and Nonlinear Control*, 2014.

[21] K. Fathian, D. I. Rachinskii, M. W. Spong, and N. R. Gans, "Globally asymptotically stable distributed control for distance and bearing based multi-agent formations," in *American Control Conference*, 2016, pp. 4642–4648.

[22] K. Fathian, D. I. Rachinskii, T. H. Summers, and N. R. Gans, "Distributed control of cyclic formations with local relative position measurements," in *IEEE Conference on Decision and Control*, 2016, pp. 49–56.

[23] K. Fathian, D. I. Rachinskii, T. H. Summers, M. W. Spong, and N. R. Gans, "Distributed formation control under arbitrarily changing topology," in *American Control Conference*, 2017, pp. 271–278.

[24] H. G. de Marina, B. Jayawardhana, and M. Cao, "Distributed algorithm for controlling scale-free polygonal formations," *IFAC-PapersOnLine*, vol. 50, no. 1, pp. 1760–1765, 2017.

[25] T. Han, Z. Lin, R. Zheng, and M. Fu, "A barycentric coordinate-based approach to formation control under directed and switching sensing graphs," *IEEE Transactions on cybernetics*, vol. 48, no. 4, pp. 1202–1215, 2018.

[26] D. V. Dimarogonas and K. H. Johansson, "Further results on the stability of distance-based multi-robot formations," in *American Control Conference*. IEEE, 2009, pp. 2972–2977.

[27] M.-A. Belabbas, "On global stability of planar formations," *IEEE Transactions on Automatic Control*, vol. 58, no. 8, pp. 2148–2153, 2013.

[28] M. H. Trinh, V. H. Pham, M.-C. Park, Z. Sun, B. D. Anderson, and H.-S. Ahn, "Comments on "Global stabilization of rigid formations in the plane"," *Automatica*, vol. 77, pp. 393–396, 2017.

[29] M.-C. Park, Z. Sun, B. D. Anderson, and H.-S. Ahn, "Distance-based control of Kn formations in general space with almost global convergence," *IEEE Transactions on Automatic Control*, 2017.

[30] L. Wang, Z. Han, and Z. Lin, "Realizability of similar formation and local control of directed multi-agent networks in discrete-time," in *IEEE Conference on Decision and Control*, 2013, pp. 6037–6042.

[31] K. Fathian, T. H. Summers, and N. R. Gans, "Robust distributed formation control of agents with higher-order dynamics," *IEEE Control Systems Letters*, vol. 2, no. 3, pp. 495–500, 2018.

[32] K. Fathian, S. Safaoui, T. H. Summers, and N. R. Gans, "Robust distributed planar formation control for higher-order holonomic and nonholonomic agents," *arXiv preprint, arXiv:1807.11058*, 2018.

[33] B. D. Anderson, C. Yu, B. Fidan, and J. M. Hendrickx, "Rigid graph control architectures for autonomous formations," *IEEE Control Systems Magazine*, vol. 28, no. 6, pp. 48–63, 2008.

[34] R. A. Horn and C. R. Johnson, *Matrix analysis*. Cambridge university press, 1990.

[35] H. K. Khalil, "Noninear systems," *Prentice-Hall, New Jersey*, vol. 2, no. 5, pp. 5–1, 1996.

[10] The "almost" global stability is due to $p_{11} = 0$, which corresponds to coinciding agents and is an unstable equilibrium.